AIP Applied Physics Letters

Remarkable differences in photoluminescent properties between LaPO4:Eu one-dimensional nanowires and zero-dimensional nanoparticles

Hongwei Song, Lixin Yu, Shaozhe Lu, Tie Wang, Zhongxin Liu et al.

Citation: Appl. Phys. Lett. **85**, 470 (2004); doi: 10.1063/1.1773616

View online: http://dx.doi.org/10.1063/1.1773616

View Table of Contents: http://apl.aip.org/resource/1/APPLAB/v85/i3

Published by the American Institute of Physics.

APPLIED PHYSICS LETTERS VOLUME 85, NUMBER 3 19 JULY 2004

Remarkable differences in photoluminescent properties between $LaPO_4:Eu$ one-dimensional nanowires and zero-dimensional nanoparticles

Hongwei Song,[a] Lixin Yu, Shaozhe Lu, Tie Wang, Zhongxin Liu, and Linmei Yang
Key Laboratory of Excited State Physics, Changchun Institute of Optics, Fine Mechanics and Physics, Chinese Academy of Sciences, Changchun 130033, People's Republic of China

(Received 6 January 2004; accepted 27 May 2004)

Photoluminescent properties of zero-dimensional $LaPO_4:Eu$ nanoparticles (NPs) and one-dimensional nanowires (NWs) prepared by the same wet-chemical synthesis technique were studied and compared. The results indicate that in NP Eu^{3+} occupied only one site, *A*, while in NW Eu^{3+} occupied the same site, *A* and an additional site *B* due to crystal anisotropy. Furthermore, the electronic transition rate of $^5D_1-\Sigma_J\ ^7F_J$ in the NW increased from 14.9 to $28.9\ \mathrm{ms}^{-1}$ compared to the NP, while the nonradiative transition rate of $^5D_1-^5D_0$ decreased from 24.1 to $19.7\ \mathrm{ms}^{-1}$. The luminescent quantum efficiency thus improved from 30% to 59%. This work demonstrates that a one-dimensional NW may be a more favorable device than a zero-dimensional NP for photoluminescence. © *2004 American Institute of Physics*. [DOI: 10.1063/1.1773616]

Recently, one-dimensional (1D) devices such as nanowires (NWs) and nanotubes have received extensive attention in both fundamental and applied studies.[1–3] They not only play a crucial role in important future optoelectronic devices,[2,4] data storage,[5] and biochemical and chemical sensors,[6] but also can be used to enrich our understanding of basic quantum mechanics.[7]

Rare earth compounds have been extensively applied to high-performance magnets, luminescence devices, catalysts, and other functional materials. Most of these functions depend strongly on the composition and structure. In the past decade, rare earth doped zero-dimensional nanoparticles (NPs) have been widely studied due to their potential application in lighting and high resolution displays.[8–10] Recently, rare earth doped one-dimensional devices such as $LaPO_4:RE$ ($RE=Eu^{3+}$, Tb^{3+}) NWs[11] and $Y_2O_3:RE$ nanotubes[12,13] and their spectroscopic properties have also attracted considerable interest. However, until now, their luminescent properties were not well compared to the zero-dimensional NPs. To develop one-dimensional phosphors, a basic question should be answered, Could the photoluminescent properties of one-dimensional devices be improved compared to zero-dimensional ones?

Bulk $LaPO_4$ is a well-known host for lanthanide ions and the Eu^{3+} ion is a sensitive activator to study local symmetry.[14,15] In this letter, we demonstrate the remarkable structural and spectral differences between $LaPO_4:Eu$ nanowires and nanoparticles. It is exciting to observe that the quantum efficiency (QE) of Eu^{3+} in NWs is enhanced twofold compared to a corresponding NP.

The $LaPO_4:Eu$ NP and NW were both prepared by the wet-chemical synthesis technique, which was reported by H. Meyssamy *et al.*[11] In the preparation of NP, appropriate amounts of high purity La_2O_3 and Eu_2O_3 (1:0.05 mol ratio) were dissolved in concentrated HNO_3 first. Then the appropriate volume of NaOH aqueous solution (0.05 M) and $(NH_4)_2HPO_4$ aqueous solution (0.18 M) were added to the solution. The final *p*H value was adjusted to 12–13 with NaOH solution (4 M). After being well stirred, a milky colloid solution was obtained and poured into several closed Teflon-lined autoclaves and subsequently heated at 120 °C for 3 h. The suspension was then centrifuged at 2770 G for 15 min and supernatant was discarded. Then, the precipitate was dissolved in dilute HNO_3 solution and the *p*H value was adjusted to 1.0. The mixture was stirred for 3 h in order to dissolve $La(OH)_3$. The white suspension obtained was centrifuged at 2770 G for 15 min. The colorless supernatant including the by-products was discarded. In order to separate NPs from micrometer particles, an appropriate amount of de-ionized water was added to the white precipitate by stirring and then centrifuged at 2770 G for 10 min, the supernatant obtaining NP were decanted. This process was repeated four times. The resultant colloidal solution was dried at 50 °C in vacuum. In the preparation of the NW, appropriate amounts La_2O_3 and Eu_2O_3 were dissolved in concentrated HNO_3 and an appropriate volume of de-ionized water was added to it. $(NH_4)_2HPO_4$ aqueous solution (0.20 M) was added to the above solution. The *p*H value of the resultant solution was adjusted to 1.0 with dilute HNO_3(1.0 M) solution. Other procedures were the same as the preparation of NP.

In measurements of fluorescent dynamics and high-resolution spectra, the sample was put into a cryostat under vacuum, in which the temperature varied from 10 to 300 K. A fourth-harmonic generator pumped by the pulsed Nd:YAG laser (line width: $1.0\ \mathrm{cm}^{-1}$, pulse duration: 10 ns, repetition frequency: 10 Hz) or a Rodamine 6G dye laser pumped by the same laser was used as the excitation source. The spectra were recorded by a Spex-1403 spectrometer, a photomultiplier, and a boxcar integrator and processed by a computer.

Figure 1 shows transition electron microscopy (TEM) images of $LaPO_4:Eu$ nanomaterials. The morphology of the particles is strikingly different for the two preparation methods: colloids prepared in strongly alkaline comprise NPs ranging in size from about 10 to 20 nm, while the preparation in acidic solution yields NWs having a width of 10–20 nm and length of 0.5–1.0 μm. Figure 2 shows an x-ray diffraction (XRD) pattern of the nanocrystalline powders. Like the bulk $LaPO_4$ polycrystals, the crystal structures

---

[a] Author to whom correspondence should be addressed; electronic mail: songhongwei2000@sina.com

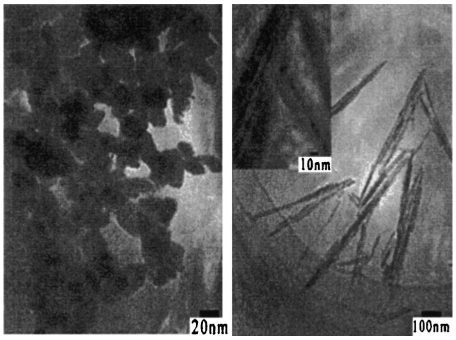

FIG. 1. TEM micrographs of the $LaPO_4$:Eu NP and NW.

of NPs and NWs both belong to monoclinic monazite type. Due to crystalline anisotropy, the relative intensity of some XRD patterns had obvious variation in NPs and NWs.

Figure 3 presents $^5D_0-^7F_J$ $(J=2,\ 1,\ 0)$ high-resolution emission spectra under 266 nm excitation in NPs and NWs [at 10 K and room temperature (RT)]. It can be seen that the room temperature spectra for the NPs and NWs are nearly same. The transition energies of the peaks have been calculated and are in good agreement with the spectral positions observed in the bulk material and Ref. 11. This suggests that the europium site in NPs and NWs has C_1 symmetry, like bulk $LaPO_4$:Eu. The spectra at low temperature in NW and NP demonstrated remarkable differences. In the NPs, three $^5D_0-^7F_1$ lines were observed, at $17\,026\pm2\ \text{cm}^{-1}$ (L1), $16\,984\pm2\ \text{cm}^{-1}$ (L2), and $16\,820\pm2\ \text{cm}^{-1}$ (L3), respectively. In the NW, besides the same lines, 1–3, three additional lines, 4–6, were observed at $16\,716\pm2\ \text{cm}^{-1}$ (L4), $16\,760\pm2$ (L5) cm^{-1}, and $16\,958\pm2\ \text{cm}^{-1}$ (L6), respectively. As is well known, the $^5D_0-^7F_1$ transitions are supersensitive to the local structure. $^7F_1$ associated with one site symmetry can split into three levels in the crystal field. The above results indicate that in NPs the $^5D_0-^7F_1$ transitions came from one site, *A*, while in NWs the $^5D_0-^7F_1$ transitions came from the same site, *A*, and an additional, *B*. It is interesting to point out that for the NW, as the preparation temperature was increased, the width increased more rapidly than that of the length and thus the crystal anisotropy decreased. In this case, sites *A* and *B* were still observed in the high-resolution spectra, but the relative emission intensity of site *B* became weaker than that of site *A*. This strongly suggests that the appearance of the additional site *B* is due to improved crystal anisotropy.

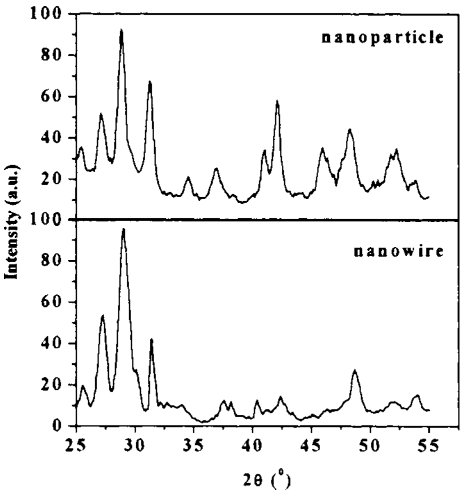

FIG. 2. XRD patterns of $LaPO_4$:Eu NPs and NWs.

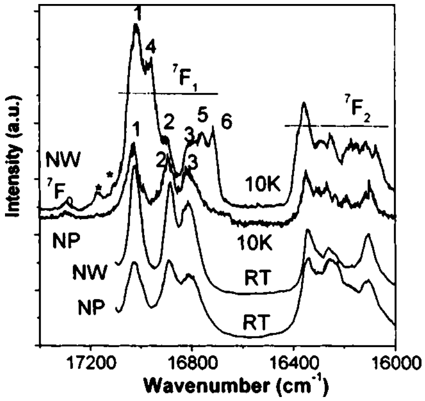

FIG. 3. High-resolution spectra of $^5D_0-^7F_J$ $(J=0,1,2)$ transitions in a $LaPO_4$:Eu NP and NW. The lines labeled by asterisks are associated with the $^5D_1-^7F_J$ transitions, which were distinguished by time-resolved spectra.

In Fig. 3, the low temperature lines of $^5D_0-^7F_2$ also demonstrated obscure differences between the NP and NW, thus site-selective spectroscopy was studied. Figures 4(a) and 4(b) show, respectively, the $^7F_0-^5D_0$ excitation spectra monitoring different $^5D_0-^7F_2$ sites and the $^5D_0-^7F_2$ emission spectra selective exciting $^7F_0-^5D_0$ transitions. In Fig. 4(a), two different excitation peaks were observed, at $\sim17\,281$ and $\sim17\,258\ \text{cm}^{-1}$, respectively. They had a little shift with the monitoring location. Corresponding to site-selective excitation, two groups of emission peaks of $^5D_0-^7F_2$ appeared, indicating that the $^5D_0-^7F_2$ transitions in the NW originated from two different sites. Site-selective spectroscopy was also performed in the NP, in which only one site was observed.

The electronic transition of Eu^{3+} in NPs and NWs was also compared. Under excitation of the 266 nm pulsed laser, electrons from ground states were excited to CTS first, and then were feed to excited ^5D_J states. The electrons in $^5D_1$ came from the nonradiative CTS feeding and the $^5D_2-^5D_1$ relaxation. The CTS feeding of ^5D is faster than the decay of ^5D. Assume that the depopulation processes in $^5D_1$ were

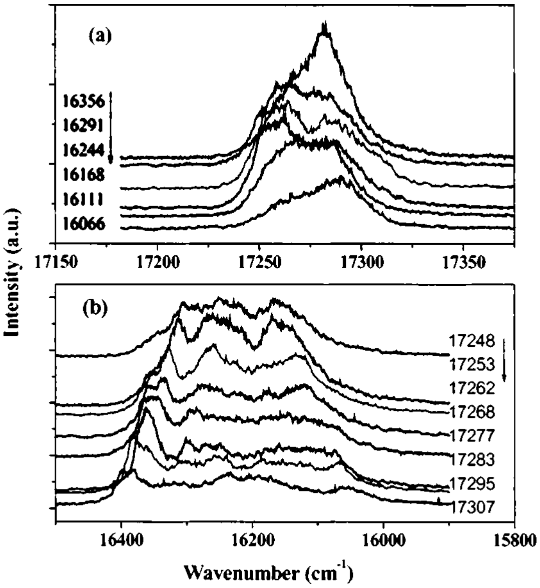

FIG. 4. Excitation spectra of $^7F_0-^5D_0$ monitoring different $^5D_0-^7F_2$ emission sites (a) and $^5D_0-^7F_2$ emission spectra exciting different $^7F_0-^5D_0$ positions (b).

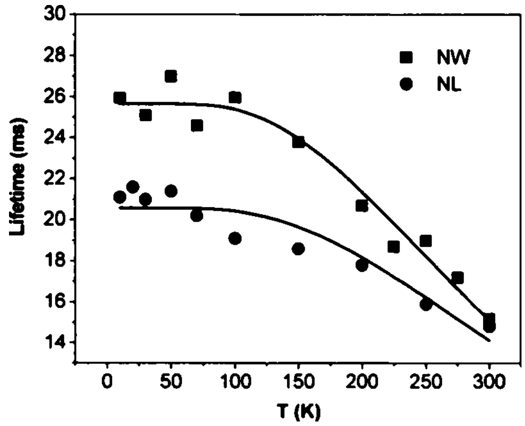

FIG. 5. Temperature dependence of the fluorescence lifetime of $^5D_1-^7F_2$ in a LaPO$_4$:Eu NP and NW (18 740 cm^{-1}). The dots are experimental data and the lines are fitting functions. Inset: Emission of the $^5D_1-^7F_1$ transitions. Inset: $^5D_1-^7F_J$ transitions in a NP.

contributed mainly by the radiative $^5D_1-\Sigma_J\,^7F_J$ transitions, and one-step nonradiative $^5D_1-^5D_0$ relaxation and the nonradiative relaxation is a multiphonon process, then the lifetime of $^5D_1$ was deduced as[16]

$$\tau_1 = \frac{1}{W_1 + W_{10}(0)[1 - e^{-h\omega/kT}]^{-\Delta E_{10}/h\omega}}, \tag{1}$$

where W_1 is the radiative transition rate of $^5D_1-\Sigma_J\,^7F_J$, $W_{10}(0)$ is the nonradiative transition rate at 0 K, ΔE_{10} is the average energy separation from $^5D_1$ to $^5D_0$, $h\omega$ is the phonon energy, k is the Boltzmann constant, and T is the absolute temperature. Figure 5 shows the fluorescence lifetime of $^5D_1-^7F_2$ as a function of the temperature. As shown, the experimental data in different samples fit well with Eq. (1). In the fitting, we chose $h\omega=390$ cm^{-1} (one of the vibrational peaks was observed at 390 cm^{-1} by Raman scattering), and $\Delta E_{10}=1758$ cm^{-1}. By fitting, W_1 and $W_{10}(0)$ were deduced as 14.9 and 24.1 ms^{-1} in the NP and 28.9 and 19.7 ms^{-1} in the NW, respectively. In comparison with the NP, the radiative transition rate in the NW increased nearly twofold, while the nonradiative transition rate decreased a little. Thus the QE improved from 30% to 59%.

For f-electron states of rare earth ions, the diameter of the electronic wave function is of the order of 10^{-1} nm, which is much smaller than the particle diameter. The size confinement effect does not work. The improved electronic transition rate in the NW was interpreted by the equation for the radiative fluorescence lifetime as follows:

$$\tau_R \approx \frac{1}{f(\mathrm{ED})}\frac{\lambda_0^2}{[1/3(n^2+2)]^2 n}, \tag{2}$$

where f (ED) is the oscillator strength for the electronic dipole transition, λ_0 is the wavelength in vacuum, and n is the refractive index of the material. In nanowires, the improved crystal anisotropy leads to an electronic dipole which is forbidden to be dissolved further and f (ED) to be improved. In addition, Meltzer *et al.*[17] observed that the radiative fluorescence lifetime of the Y$_2$O$_3$:Eu NP is dependent not only on the refractive index itself, but also on the surrounding medium. They deduced that, in nanoparticles, n in Eq. (2) should be substituted by the effective refractive index $n_{\mathrm{eff}}=xn+(1-x)n_{\mathrm{med}}$, where x is the filling factor, showing what fraction of space is occupied by the nanoparticles and n_{med} is the refractive index of the surrounding media.[17] In the present case, the samples were surrounded by vacuum, thus $n_{\mathrm{med}}=1$. Based on the definition of x, it is believed that the value of x for the NW is larger than that for the NP, leading to the increase of n_{eff} and the decrease of the radiative fluorescence lifetime.

In conclusion, the structural and luminescent properties of colloidal LaPO$_4$:Eu^{3+} NWs and NPs prepared by the same technique were studied and compared. In NPs, Eu^{3+} occupy only one site, *A*. In NWs, due to the increased crystalline anisotropy, the Eu^{3+} ions occupy two different sites, *A* and *B*. The radiative transition rate of $^5D_1-\Sigma_J\,^7F_J$ and the QE in the NW increased nearly twofold in comparison to in the NP. This work is significant for developing one-dimensional nanometer phosphors.

This work was financially supported by the One Hundred Talent Project of the Chinese Academy of Sciences and by the National Science Foundation (Grant No. 10374086).

[1] S. Lijima, Nature (London) **354**, 56 (1991).
[2] X. F. Daun, Y. Huang, Y. Cui, J. F. Wang, and C. M. Lieber, Nature (London) **409**, 66 (2001).
[3] E. C. Dickey, C. A. Crimes, M. K. Jain, K. G. Ong, D. Qian, P. D. Kichambare, R. Andrews, and D. Jacques, Appl. Phys. Lett. **79**, 4022 (2001).
[4] H. Kind, H. Yan, M. Law, B. Messer, and P. Yang, Adv. Mater. (Weinheim, Ger.) **14**, 158 (2002).
[5] Y. C. Kong, D. P. Yu, B. Zhang, W. Fang, and S. Q. Feng, Appl. Phys. Lett. **78**, 4 (2001).
[6] Y. Cui, Q. Wei, H. Park, and C. M. Lieber, Science **299**, 1874 (2003).
[7] D. D. Ma, C. S. Lee, F. C. K. Au, S. Y. Tong, and S. T. Lee, Science **293**, 1289 (2003).
[8] D. Matsuura, Appl. Phys. Lett. **81**, 4526 (2002).
[9] Z. Wei, L. Sun, C. Liao, and C. Yan, Appl. Phys. Lett. **80**, 1447 (2002).
[10] K. Riwotzki, H. Meyssamy, A. Kornowski, and M. Hasse, J. Phys. Chem. **104**, 2824 (2000).
[11] H. Meyssamy, K. Riwotzki, A. Kornowski, S. Naused, and M. Haase, Adv. Mater. (Weinheim, Ger.) **11**, 840 (1999).
[12] M. Yada, M. Mihara, S. Mouri, and T. Kijima, Adv. Mater. (Weinheim, Ger.) **14**, 309 (2002).
[13] C. Wu, W. Qin, G. Qin, D. Zhao, J. Zhang, and S. Huang, Appl. Phys. Lett. **82**, 520 (2003).
[14] W. L. Wanmaker, A. Bril, J. W. T. Vrugt, and J. Broos, Philips Res. Rep. **21**, 270 (1966).
[15] R. D. Peacock, Struct. Bonding (Berlin) **22**, 83 (1975).
[16] H. Song, J. Wang, B. Chen, and S. Lu, Chem. Phys. Lett. **376**, 1 (2003).
[17] R. S. Meltzer, S. P. Feofilov, B. Tissue, and H. B. Yuan, Phys. Rev. B **60**, R14012 (1999).